ELSEVIER

Catalysis Today 70 (2001) 383–391

CATALYSIS TODAY

www.elsevier.com/locate/cattod

Spatiotemporal patterns in models of cross-flow reactors

Moshe Sheintuch*, Olga Nekhamkina

Department of Chemical Engineering, Technion — Israel Institute of Technology, Technion City, Haifa 32 000, Israel

Abstract

We review the behavior of stationary and moving spatially periodic patterns in a simple cross-flow fixed-bed reactor with a first-order exothermic reaction subject to the Danckwert's boundary conditions and realistically high *Le* and *Pe*. Spatiotemporal patterns emerge due to the interaction of concentration and temperature balances, much like dynamic patterns in a CSTR. Moving waves emerge in an unbounded system, but they transform into stationary spatially inhomogeneous patterns in a bounded system above certain *Pe* threshold. The critical parameters of this threshold are derived analytically. A weakly nonlinear analysis is used in order to derive the governing amplitude equation.

The spatial behavior in the bounded system with $Pe \to \infty$ is analogous to the temporal behavior of the simple thermokinetic CSTR problem and the behavior of the distributed system is classified according to that of the lumped one. Both regular kinetics and oscillatory one (with reversible catalytic activity) are considered. Suggestions for experimental realization of these phenomena are discussed.

Keywords: Spatiotemporal patterns; Moving and standing waves; Reactor

1. Introduction

The purpose of this work is to review the rich plethora of spatiotemporal patterns, that may emerge in a catalytic reactor with dispersion of a reactant along the bed. Such dispersion of the feed rather than supplying it with the feed, may be advantageous in several classes of reactions. Dispersing the feed along the reactor in reactions with self-inhibition, we may maintain the reactant concentration at its optimal concentration, a value that leads to a maximal rate. Gradual feeding of oxygen may improve selectivity in partial-oxidation reactions [12], where high feed concentration leads to poor selectivity, while low concentration limits the rate and conversion. Such supply can be fixed at discrete ports or, with the help of selective membranes, distributed continuously along the reactor. Mass supply and heat removal require two interfaces within the reactor. These can be organized as an annular tube with mass-transfer at one wall and heat-transfer at the other or as a multitube reactor incorporating two kinds of tubes for the two transfer processes.

In series of works [5–7], we have recently analyzed patterns in a cross-flow reactor including standing or moving waves and aperiodic patterns which emerge due to a first-order exothermic reaction with realistic (Danckwert's) boundary conditions and with $Le \gg 1$, $Pe \gg 1$. In previous studies of spatiotemporal patterns in heterogeneous and homogeneous models of a fixed-bed reactor, using the generic first-order Arrhenius kinetics [9,10] or a detailed multistep model, like the one that applies to CO oxidation in the catalytic converter (see the previous paper in this issue), patterns emerge due to interaction of kinetics or thermal bistability with a slow reversible change

* Corresponding author. Tel.: +972-4-8292823; fax: +972-4-8230476.
E-mail address: cermsll@tx.technion.ac.il (M. Sheintuch).

0920-5861/01/$ – see front matter
PII: S0920-5861(01)00345-5

Nomenclature

B	dimensionless exothermicity
c_p	volume-specific heat capacity
C	key component concentration
D	axial dispersion coefficient
Da	Damkohler number
E	activation energy
ΔH	reaction enthalpy
k	thermal conductivity
L	reactor length
Le	Lewis number
Pe	Peclet number
r	reaction rate
t	time
T	temperature
u	fluid velocity
x	dimensionless concentration
y	dimensionless temperature

Greek symbols

α_T, α_C	heat and mass transfer coefficients
ϵ	bed void fraction
ρ	density

Subscripts

e	efficient value
f	fluid
in	at the inlet
s	solid
w	wall value

in activity. Patterns in a cross-flow reactor do not require such a slow inhibitor and may emerge even in the case of the constant catalytic activity. The unique aspect of a cross-flow reactor is that sufficiently far from the inlet the system approaches a homogeneous (space-independent) solution. Spatiotemporal patterns emerge due to the interaction of concentration and temperature balances, much like dynamic patterns in a CSTR. Highly exothermic or highly activated reactions may yield multiple homogeneous solutions and in the distributed system fronts separating different states may be formed. Moreover, even in the case when only a single steady state exists a rich plethora of patterns may be sustained and they bifurcate with a finite wavelength from the homogeneous state. Similar results were obtained by Andresén et al. [1] and Kuznetsov et al. [4] for a learning Brusselator model, and by Satnoianu and Menzinger [8] for Gray–Scott kinetics that admit a single steady state solution.

The structure of the review is as follows. In the next section, we simulate and analyze the behavior of spatially periodic patterns in an unbounded system and derive the analytical expressions for the critical parameters (Pe_0, k_0) of the stationary patterns excitation. We then study a finite-size reactor subject to the Danckwert's boundary conditions. We also draw the analogy between the stationary spatially oscillated patterns in the distributed system and temporal patterns in the simple CSTR problem. As claimed earlier emergence of this behavior does not require an oscillatory kinetics (i.e., Hopf bifurcation), or different diffusivities (Turing bifurcation) or even differential bulk flow. We also study the effect of the oscillatory kinetics by coupling the thermokinetic model with a slow process of changing the catalytic activity to find out whether it introduces new features. Nonlinear analysis is presented in Section 4.

2. Reactor models and linear analysis

We employ a conventional homogeneous model of a fixed-bed reactor with terms describing heat loss due to cooling ($\alpha_T(T - T_w)$) and mass supply through a membrane wall ($\alpha_C(C - C_w)$). For the 1D case, the appropriate system equations with negligible dispersion of mass and first-order activated kinetics, $r = A\varphi \exp(-E/RT)C$ takes the following dimensionless form (see [10]):

$$\frac{\partial x}{\partial \tau} + \frac{\partial x}{\partial \xi} = Da\,\varphi(1-x)\exp\left(\frac{\gamma y}{\gamma + y}\right) - \alpha_C(x - x_w) = f(x, y),$$

$$Le\frac{\partial y}{\partial \tau} + \frac{\partial y}{\partial \xi} - \frac{1}{Pe}\frac{\partial^2 y}{\partial \xi^2} = B\,Da\,\varphi(1-x)\exp\left(\frac{\gamma y}{\gamma + y}\right) - \alpha_T(y - y_w) = g(x, y) \quad (1)$$

subject to the Danckwert's boundary conditions

$$\xi = 0, \quad x = 0, \quad \frac{1}{Pe}\frac{\partial y}{\partial \xi} = y, \quad \xi = \tilde{L}, \quad \frac{\partial y}{\partial \xi} = 0. \quad (2)$$

Here conventional notations are used with

$$x = 1 - \frac{C}{C_{\text{in}}}, \quad y = \gamma \frac{T - T_{\text{in}}}{T_{\text{in}}}, \quad \xi = \frac{z}{z_0},$$
$$\tau = \frac{tu}{z_0}, \quad \gamma = \frac{E}{RT_{\text{in}}}, \quad B = \gamma \frac{(-\Delta H)C_{\text{in}}}{(\rho c_p)_{\text{f}} T_{\text{in}}},$$
$$Da = \frac{Az_0}{u} \mathrm{e}^{-\gamma}, \quad Le = \frac{(\rho c_p)_{\text{e}}}{(\rho c_p)_{\text{f}}}, \quad Pe = \frac{(\rho c_p)_{\text{f}} z_0 u}{k_{\text{e}}} \tag{3}$$

and φ is the degree of the surface activity. Note, that we did not use the reactor length L as the length scale, but rather an arbitrary value z_0, so that $\tilde{L} = L/z_0$ can be varied as a free parameter. Conventional definitions of Pe correspond to ours $Pe\,\tilde{L}$. Typically the bed heat capacity is large ($Le \gg 1$) and $Pe \gg 1$.

In the first part of the work, we keep $\varphi = 1$. Later, we allow for varying φ. While there is no a general agreement on the source of activation or deactivation, and their rates, we adopt here a simple linear expression that assumes that deactivation occurs faster at higher temperatures and at higher activities and that it is independent of reactant concentration, so that it can be expressed by a single line in the (y, φ) phase plane [2]

$$K_\varphi \frac{\partial \varphi}{\partial \tau} = a_\varphi - b_\varphi \varphi - y = h(y, \varphi) \tag{4}$$

and typically $K_\varphi \gg 1$.

2.1. Constant activity case

The solutions of the right-hand side of Eq. (1) ($f(x_{\text{s}}, y_{\text{s}}, 1) = g(x_{\text{s}}, y_{\text{s}}, 1) = 0$) are the asymptotic homogeneous solutions of the problem and up to three solutions may exist within a certain set of parameters. Under these conditions, we may find fronts separating different steady states.

To understand the patterns admitted by Eqs. (1) and (2), let us review the behavior of several simplified and related systems:

1. If we ignore the heat-dispersion term then the steady state system

$$\frac{\mathrm{d}x}{\partial \xi} = f(x, y, 1), \qquad \frac{\mathrm{d}y}{\partial \xi} = g(x, y, 1) \tag{5}$$

is exactly the model describing the temporal dynamics of a homogeneous CSTR, in which an exothermic first-order reaction is conducted. The analysis of sustained motions of the CSTR (Eq. (5)) is useful in describing and classifying the behavior of a long reactor. This problem has been investigated extensively for the case of the constant catalytic activity in order to map the various bifurcation diagrams and phase planes in the parameter space (e.g., [3,13,14]).

2. The steady state solution is described by

$$\frac{\mathrm{d}x}{\partial \xi} = f(x, y, \varphi(y)), \quad \frac{\mathrm{d}y}{\partial \xi} = p,$$
$$\frac{\mathrm{d}p}{\partial \xi} = Pe(p - g(x, y, \varphi(y)). \tag{6}$$

The multiplicity patterns of this system are identical to those of Eq. (5), but the new term affects the dynamics. Hopf bifurcation occurs when the eigenvalues (m_i) of the Jacobian matrix are imaginary, $m_{1,2} = \pm \mathrm{i}k_0$ or

$$k_0 = (-f_x^2 - g_x f_y)^{1/2}, \qquad Pe_0 = \frac{k_0^2}{f_x + g_y}. \tag{7}$$

3. We conducted a linear stability analysis of the full system (1) in an infinitely long region which is not affected by the boundaries or in a ring-shaped system. Denoting the deviation from the basic steady state solution $\mathbf{u}_0 = \{x_{\text{s}}, y_{\text{s}}\}$ as $\mathbf{u}_1 = \{x_1, y_1\}$, we arrive at the following system for the perturbations:

$$\frac{\partial \mathbf{u}_1}{\partial \tau} - \mathbf{V} \frac{\partial \mathbf{u}_1}{\partial \xi} - \mathbf{D} \frac{\partial^2 \mathbf{u}_1}{\partial \xi^2} = \mathbf{J}\mathbf{u}_1, \tag{8}$$

where $\mathbf{D} = \text{diag}\{0, (Le\,Pe)^{-1}\}$, and $\mathbf{V} = -\text{diag}\{1, Le^{-1}\}$ are the diffusion and convection matrices. Assuming the perturbations $\mathbf{u}_1 = \{x_1, y_1\} \sim \mathrm{e}^{\mathrm{i}k\xi + \sigma\tau}$, where k is the perturbation wave number and σ is the time growth rate, and using it in (8), we obtain the dispersion relation $\mathcal{D}(\sigma, k) = 0$. The bifurcation condition $\text{Re}\,\sigma = 0$ defines the neutral curve, that may be calculated numerically for a chosen set of parameters. We used Pe as the bifurcation parameter as it does not influence the steady states solutions. Moreover, the stationary patterns emerging at $Pe \to \infty$ for the system (1) correspond to the dynamic behavior of the corresponding CSTR problem. The neutral curve typically acquires a minimum (ω_{c}, Pe_{c}, see Fig. 1) and crossing Pe_{c} corresponds to an

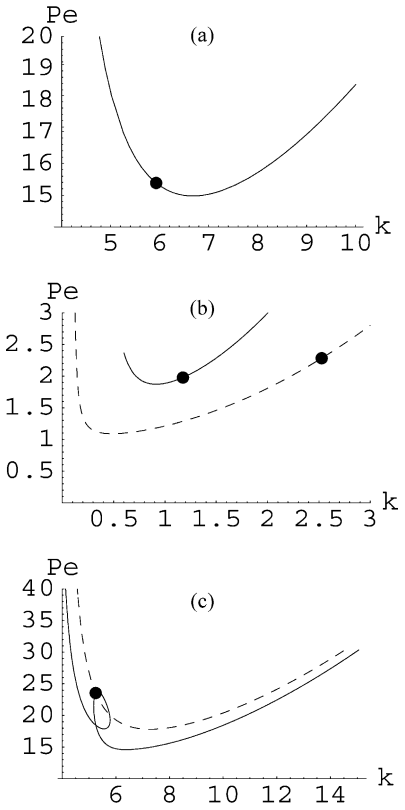

Fig. 1. Neutral curves: (a) $\varphi \equiv 1$, $B = 16.2$, $\alpha = 4$, $Da = 0.2$; (b) $\varphi \equiv 1$, $B = 16.2$, $\alpha = 4$, $Da = 0.132$, the solid and dash lines correspond to the lower and upper steady state solutions; (c) varying φ case with $a_\varphi = B$, $K_\varphi = 10^4$ (solid line) or $K_\varphi = 10^2$ (dash line; other parameters as in (a)). The dot denotes the amplification threshold (Pe_0, k_0) (after Nekhamkina et al. [7]).

excitation of oscillatory solutions with finite k in an unbounded system moving at a constant speed.

Note that Yakhnin et al. [15–17] in their investigation of the differential flow induced chemical instability (DIFICI), applied linear stability analysis to "ring-shaped" reactors with periodic boundary conditions or to "linear" reactors with special boundary conditions that maintain the homogeneous solution. Patterns were found to emerge when the magnitude of the differential bulk flow of concentration and temperature exceeds a critical value, i.e., above the convective instability threshold. They simulated traveling wave trains but did not observed the stationary patterns, as the stationary perturbation threshold ($Pe = Pe_0$) was not exceeded in these studies.

4. Let us consider now the bounded system governed by Eq. (1) with the applied boundary conditions (2). As was demonstrated in [5], the moving patterns predicted in the infinite region are suppressed by the boundaries and above some threshold *Pe* are transformed into *stationary patterns*, which generally do not correspond to the minimum of the neutral curve. For such patterns to emerge, we should impose a condition of zero frequency $\omega = 0$ in addition to the relation $\mathrm{Re}\,\sigma = 0$. If both of these conditions are matched, we may determine a threshold value for amplification of the stationary perturbation (see Fig. 1). Its coordinates are identical to the Hopf bifurcation point for Eq. (6), i.e., defined by Eq. (7), but k_0 now is the spatial wave number.

2.2. Variable catalytic activity case

The analysis presented above may be applied to the full model that accounts for reversible changes of the catalytic activity. In the limit of large Peclet numbers $Pe \to \infty$, the steady state solutions of the full systems (1) and (4), if they exist, are fully equivalent to the temporal solution of the corresponding CSTR model with the modified kinetics:

$$\frac{\partial x}{\partial \tau} = f(x, y, \varphi), \quad \frac{\partial y}{\partial \tau} = g(x, y, \varphi), \quad \varphi = \frac{a_\varphi - y}{b_\varphi}. \tag{9}$$

The critical parameters k_0, Pe_0 in this case can be determined by formulas (7) as well, using the gain differentiating rule for functions $f(x, y, \varphi(y))$ and $g(x, y, \varphi(y))$ with $\varphi(y)$ defined by (9).

To simplify the following analysis, we used a_φ as a free parameter and define $b_\varphi = a_\varphi - y_s$, in order to ensure the same set of the steady state solution of the two-variable system (y_s, x_s) to be the solution of the full system with $\varphi_s = 1$.

The form of the neutral curve drastically depends on the parameters $K_\varphi, a_\varphi, b_\varphi$. For $a_\varphi \gg y_s$ and $K_\varphi \sim Le$ the neutral curve (Fig. 1c, dash line) is shifted but preserve the same form as for the constant activity case. With increasing K_φ the neutral curve changes significantly (compare the solid and dash lines in Fig. 1c), but the critical values Pe_0, k_0 corresponding to

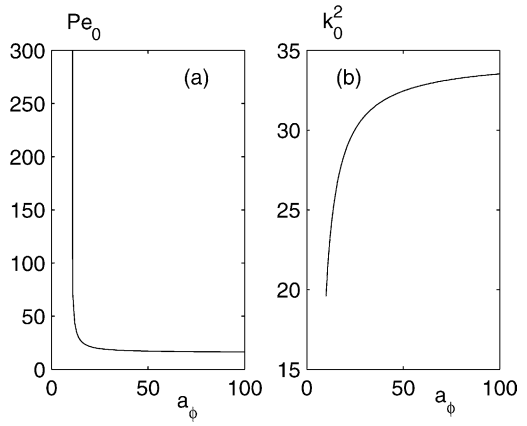

Fig. 2. Dependence of the critical parameters Pe_0 (a) and k_0 (b) on the activity variation parameter a_φ, $K_\varphi = 100$, $b_\varphi = a_\varphi - y_s$, $B = 16.2$, $\beta = 3$, $Da = 0.2$ (after Nekhamkina et al. [7]).

emergence of the stationary patterns obviously do not depend on the time scales.

Typical dependences of Pe_0, k_0 on a_φ are plotted in Fig. 2a and b. With $a_\varphi \to \infty$, $\varphi_s \to 1$ and the critical parameters tends to the asymptotic values corresponding to the case of regular kinetics.

3. Numerical simulations

We consider below two sets of parameters with fixed activity $\varphi = 1$ to demonstrate the dynamics. Other cases are considered in [5,6]. We then study the effect of varying φ.

3.1. Regular kinetics

Case 1 ($\varphi = 1$). The simplest CSTR dynamics is one that admits an unstable steady state solution surrounded by a stable limit cycle. The corresponding neutral curve typically acquires the form of Fig. 1a and includes a bifurcation point. For $Pe > Pe_c$, the system exhibits transients of traveling waves: once excited they move until they are consequently arrested near the boundaries. In the subcritical region ($Pe_c < Pe < Pe_0$), the amplitude of the wavy patterns decays along the reactor.

Stationary space-periodic patterns are established for $Pe > Pe_0$. The amplitude of these patterns varies in space but tends to some saturated value, as it follows from the nonlinear stability analysis. For relatively small deviations from the bifurcation the patterns have an harmonic form and the computed wave number is in a very good agreement with the theoretical value k_0 (Eq. (7)). With increasing Pe, the amplitude of the state variables grows (Fig. 3). The structure of the patterns become insensitive to Pe number for large Pe and, as expected, the form of the spatial patterns completely corresponds to the dynamic behavior of the corresponding CSTR model.

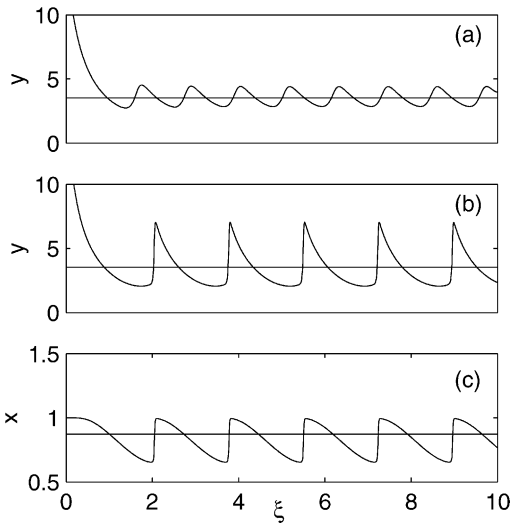

Fig. 3. Steady state profiles of the dimensionless temperature (y) (a, b) and concentration (x) (c) for $Pe = 20$ (a) and 100 (b, c). The horizontal lines show the steady state level ($\varphi \equiv 1$, Case 1, parameters as in Fig. 1a, $L = 10$) (after Nekhamkina et al. [6]).

Case 2 ($\varphi = 1$). The other case with $\varphi = 1$ to be considered here corresponds to a CSTR problem which admits three unstable steady states surrounded by a single stable limit cycle. The neutral curves calculated for the lower (x_{s1}, y_{s1}) and upper (x_{s3}, y_{s3}) steady state solutions for the full system exhibit local minima and stationary pattern bifurcation points (Fig. 1b).

For $Pe < \min(Pe_{c1}, Pe_{c3})$ only stationary solutions, depending on the initial conditions are obtained. In a domain, which roughly lies around the two critical Pe, the system exhibits spatiotemporal patterns (Fig. 4). At $Pe = 1.5$, a strictly periodic motion is sustained in which a single hot spot emerges somewhere within the reactor inlet, moves upstream and disappears.

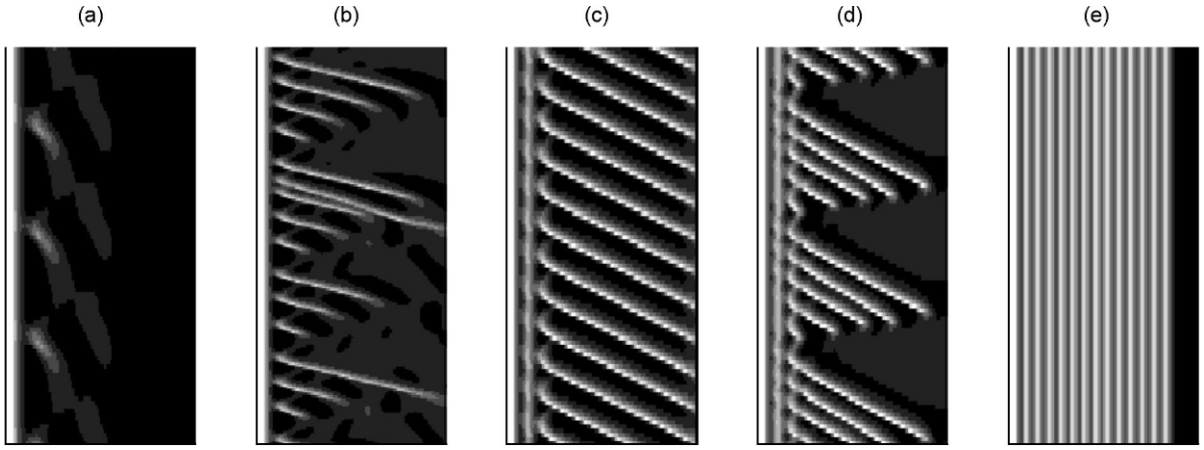

Fig. 4. Effect of *Pe* on the spatiotemporal patterns for Case 2 (parameters as in Fig. 1b, $L = 25$): $Pe = 1.5$ (a — periodic solution with a moving hot spot), 2.1 (b — aperiodic behavior), 3.0 (c — period-one patterns), 3.5 (d — period-5 packet), 5.0 (e — stationary patterns). (after Nekhamkina et al. [6]).

Aperiodic behavior is recorded for $Pe = 2.1$–2.3 (Fig. 4b) and the corresponding two-dimensional (2D) or 3D (with the addition of the derivative $dy/d\xi$ as a third coordinate — Fig. 5) phase-plane and phase-space exhibit a strange attractor. Regular period-5 patterns are established at $Pe = 2.5$. The short waves are consequently followed by the longer waves forming a single packet which is composed of five waves. At $Pe = 3.0$, regular moving patterns that span most of the reactor are established (Fig. 4c) The period-5 pattern is maintained again in the range $3 < Pe < 4$, but unlike the lower *Pe* regimes, a single standing wave is already formed near the inlet (compare Fig. 4b and d). Stationary patterns are established for $Pe > 5$ and eventually cover the whole region (Fig. 4e). With increasing *Pe*, as in the previous case, the standing wave patterns are significantly rearranged and for $Pe > 10^3$ become quite similar to the temporal solution of the corresponding CSTR problem.

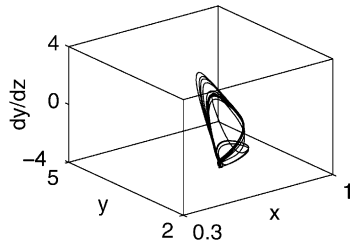

Fig. 5. The three-dimensional $(dy/d\xi, y, x)$ phase space for Case 2 plotted at $\xi = 0.25L$ and $Pe = 2.1$ (a strange attractor) (after Nekhamkina et al. [6]).

3.2. Oscillatory kinetics

The system behavior for sets of parameters that correspond to relatively small oscillations of the catalytic activity is quite similar to the constant activity case: stationary patterns emerge above the critical $Pe = Pe_0$, they are continuously transformed with increasing bifurcation parameter, and for large *Pe* the form of the

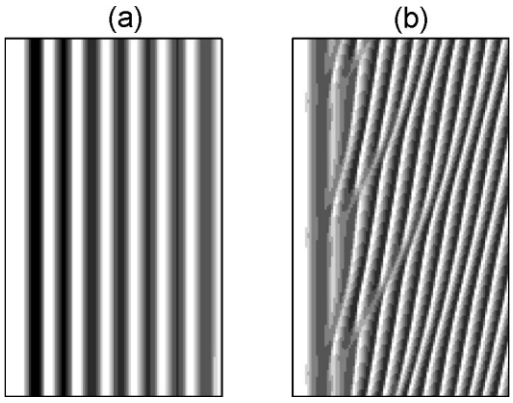

Fig. 6. Effect of the time scale on the pattern selection for the oscillatory kinetics model: stationary waves with $K_\varphi = 10^2$ (a), aperiodic moving waves with $K_\varphi = 10^4$ (b). $a_\varphi = 1.5y_s$, other parameters as in Fig. 1c (after Nekhamkina et al. [7]).

patterns completely corresponds to the dynamic behavior of the related CSTR with the modified kinetics.

With decreasing a_φ ($a_\varphi \to y_s$), the mechanism of patterns selection changes drastically. In the supercritical region, the system exhibit moving aperiodic waves which may be "arrested" by the boundaries only for relatively small deviations $\Delta Pe = Pe - Pe_0$. The range of Pe, for which the stationary patterns are established decreases with increasing K_φ (see Fig. 6). For $Pe \gg Pe_0$ a chaotic behavior was observed in many cases, but its classification is rather cumbersome and will be considered in the following work.

4. Nonlinear analysis

Nonlinear analysis may provide some general results of the system behavior, but its application is limited to an unbounded system or a system with periodic boundary conditions. While we do not present here the nonlinear analysis of the systems (1) and (4), we recall recent results of the constant activity ($\varphi \equiv 1$) case [5]. We introduced a hierarchy of time and spatial scales

$$\frac{\partial}{\partial t} = \frac{\partial}{\partial t_0} + \epsilon \frac{\partial}{\partial t_1} + \epsilon^2 \frac{\partial}{\partial t_2} + \cdots,$$

$$\frac{\partial}{\partial \xi} = \frac{\partial}{\partial \xi_0} + \epsilon^\beta \frac{\partial}{\partial \xi_1} + \cdots. \tag{10}$$

Here the value of β should be chosen to balance properly terms of different orders of ϵ ($\beta = 2$ here, see the arguments in [5]). We also expand the phase variables and the bifurcation parameter as

$$\mathbf{u} = \mathbf{u}_0 + \epsilon \mathbf{u}_1 + \epsilon^2 \mathbf{u}_2 + \cdots,$$

$$Pe = Pe_0 + \epsilon Pe_1 + \epsilon^2 Pe_2 + \cdots. \tag{11}$$

Substituting the above expansions into the original set of equations, and collecting terms of the same orders of ϵ, we produce a set of equations. The resulting amplitude equation has the following form [5]:

$$\frac{\partial a}{\partial t_2} = -c_3 |a|^2 a + c_1 a + v \frac{\partial a}{\partial \xi_1}. \tag{12}$$

Using the polar representation of the complex amplitude $a = r\,\mathrm{e}^{\mathrm{i}\phi}$, we arrive at a pair of real equations

$$\frac{\partial r}{\partial t_2} = -c_{3\mathrm{r}} r^3 + c_{1\mathrm{r}} r + v_\mathrm{r} \frac{\partial r}{\partial \xi_1} - v_\mathrm{i} r \frac{\partial \phi}{\partial \xi_1},$$

$$\frac{\partial \phi}{\partial t_2} = -c_{3\mathrm{i}} r^2 + c_{1\mathrm{i}} + \left(\frac{v_\mathrm{i}}{r}\right) \frac{\partial r}{\partial \xi_1} + v_\mathrm{r} \frac{\partial \phi}{\partial \xi_1}. \tag{13}$$

Here the subscripts r and i of the coefficients correspond to the real and imaginary parts of the corresponding quantities.

It should be emphasized that Eqs. (12) and (13) are actually ill-posed, i.e, infinitesimally small perturbations of a solution will grow very fast, so that the original approximation is no longer justified. However, these equations are useful for analysis of two different cases:

1. When the spatial modulation of the amplitude is neglected ($\partial a/\partial \xi_1 = 0$), thus the wave number is prescribed, the equations for the real amplitude r and the phase ϕ are separated. We found then that the former equation has a nontrivial stable solution

$$r_\mathrm{s} = \sqrt{\frac{c_{1\mathrm{r}}}{c_{3\mathrm{r}}}}, \quad \phi_\mathrm{s} = \frac{c_{3\mathrm{r}} c_{1\mathrm{i}} - c_{3\mathrm{i}} c_{1\mathrm{r}}}{c_{3\mathrm{r}}} t_2 = \Omega t_2. \tag{14}$$

   The later condition leads to a frequency shift Ω proportional to the parametric deviation. This implies that the perturbation has the form of traveling wave with a velocity

$$V = \frac{\Omega}{k_0}. \tag{15}$$

   The simplest way to check this regime is to simulate the reactor with periodic boundary conditions. As was demonstrated in the degenerate case, when the critical points Pe_0, k_0 and $Pe_\mathrm{c}, k_\mathrm{c}$ coincide [5], the analytical and numerical amplitudes and velocities are in a very good agreement for small deviations in ΔPe.
2. In the second case of the stationary solution with the spatially modulated amplitude ($\partial r/\partial t_2 = \partial \phi/\partial t_2 = 0$), the system (13) may be reduced to the following problem in the semi-infinite region:

$$\frac{\mathrm{d}r}{\mathrm{d}\xi_1} = r(-\tilde{c}_{3\mathrm{r}} r^2 + \tilde{c}_{1\mathrm{r}}),$$

$$\frac{\mathrm{d}\phi}{\mathrm{d}\xi_1} = (-\tilde{c}_{3\mathrm{i}} r^2 + \tilde{c}_{1\mathrm{i}}) \tag{16}$$

($\tilde{c}_3 = -c_3/v$, $\tilde{c}_1 = -c_1/v$), subjected to non-homogeneous inlet conditions. The Danckwert's boundary conditions produce, in the general case, very high perturbations, which cannot be taken into account by the weak stability analysis. The saturated amplitudes, obtained in numerical simulation preserve the linear dependence on $\sqrt{\Delta Pe}$ for small $\Delta Pe/Pe$ (5–10%), but the slope of these lines differs from the analytical values (by 20–40%) [5]. A good agreement between analytical and numerical results was obtained only using fixed values of variables at the boundaries $\mathbf{u}|_{\xi=0} = \mathbf{u}_s + \delta\mathbf{u}$ ($\delta\mathbf{u} \ll 1$) [5].

5. Concluding remarks

The patterns presented here emerge due to the interaction of reaction and convection of the activator, in contrast to Turing patterns [11] that emerge due to competition of an activator and a diffusing inhibitor in quiescent fluids. Large amplitude stationary space-periodic patterns have been simulated and analyzed for a bounded system. The linear stability analysis for this model was performed, using *Pe* as a bifurcation parameter, and the analytical expression for an amplification threshold was derived.

The stationary spatial behavior of the distributed system, in the limit case $Pe \to \infty$, formally correspond to the temporal dynamics of a homogeneous CSTR. The CSTR model will not predict oscillations in catalytic systems due to the large solid heat-capacity, but that parameter will not affect the spatial patterns presented here. Only stationary patterns emerge in the distributed system for the simplest dynamics which admits an unstable steady state solution surrounded by a stable limit cycle in a CSTR. For more complicated cases both regular and aperiodic behaviors are observed in the distributed systems which obviously cannot be predicted by the linear stability analysis.

The emerging patterns are of great academic interest, but we would like to discuss here the feasibility of their experimental realizations. As we have noted above, the phenomena will appear in thermokinetic systems that admit oscillatory behavior in their $Le = 1$ version, which applies to many oxidation, hydrogenation and other reactions. While we have analyzed the reactor with a continuous supply of reactants, a model with finite number of supply ports will also exhibit similar behavior if their number is large enough and they are placed at the crests of the emerging wave. We still need to check the engineering implications by studying a real-case example. Such designs may be aimed at supplying oxygen to a partial-oxidation reaction or coupling of endothermic dehydrogeneration and exothermic oxidation reactions in a membrane reactor.

While we employed a "generic" model to show the emergence of non-Turing stationary patterns, more realistic models will use other features as well which will be considered in future works. One modification we want to consider is the effect of a second reaction (i.e., two consecutive reactions, partial and complete oxidation) that kicks off at higher temperatures. In a CSTR such kinetics may lead to temporal chaotic behavior.

Acknowledgements

This work was supported by the Volkswagen-Stiftung Foundation. MS is a member of the Minerva Center of Nonlinear Dynamics. OA is partially supported by the Center for Absorption in Science, Ministry of Immigrant Absorption State of Israel.

References

[1] P. Andresén, M. Bache, E. Mosekilde, G. Dewel, P. Borckmanns, Stationary space-periodic structures with equal diffusion coefficients, Phys. Rev. E 60 (1999) 297.
[2] M. Barto, M. Sheintuch, Excitable waves and spatiotemporal patterns in a fixed-bed reactor, AIChE J. 40 (1994) 120.
[3] J. Guckenheimer, Multiple bifurcation problems for chemical reactors, Physica D 20 (1986) 1.
[4] S.P Kuznetsov, E. Mosekilde, G. Dewel, P. Borckmans, Absolute and convective instabilities in a one-dimensional Brusselator flow model, J. Chem. Phys. 106 (1997) 7609.
[5] O.A. Nekhamkina, A.A. Nepomnyashchy, B.Y. Rubinstein, M. Sheintuch, Nonlinear analysis of stationary patterns in convection–reaction–diffusion systems, Phys. Rev. E 61 (2000) 2436–2444.
[6] O.A. Nekhamkina, B.Y. Rubinstein, M. Sheintuch, Spatiotemporal patterns in thermokinetic models of cross-flow reactors, AIChE J. 46 (2000) 1632–1640.
[7] O.A. Nekhamkina, B.Y. Rubinstein, M. Sheintuch, Spatiotemporal patterns in models of cross-flow reactors.

Regular and oscillatory kinetics, Chem. Eng. Sci. 56 (2001) 771–778.
[8] R. Satnoianu, M. Menzinger, Non-turing stationary patterns in flow-distributed oscillators with general diffusion and flow rates, Phys. Rev. E 62 (2000) 113–119.
[9] M. Sheintuch, O. Nekhamkina, Pattern formation in homogeneous reactor models, AIChE J. 45 (1999) 398.
[10] M. Sheintuch, O. Nekhamkina, Pattern formation in homogeneous and heterogeneous reaction models, Chem. Eng. Sci. 54 (1999) 4535.
[11] A.M. Turing, The chemical basis for morphogenesis, Phil. Trans. R. Soc. B 327 (1952) 37.
[12] C. Téllez, M. Menéndez, J. Santamaría, Simulation of an inert membrane reactor for the oxidative dehydrogeneration of butane, Chem. Eng. Sci. 54 (1999) 2917.
[13] A. Uppal, W.H. Ray, A.B. Poore, On the dynamic behavior of continuous stirred tank reactors, Chem. Eng. Sci. 29 (1974) 967.
[14] A. Uppal, W.H. Ray, A.B. Poore, The classification of the dynamic behavior of continuous stirred tank reactors—influence of reactor residence time, Chem. Eng. Sci. 31 (1976) 205.
[15] V.Z. Yakhnin, A.B. Rovinsky, M. Menzinger, Differential flow instability of the exothermic standard reaction in a tubular cross-flow reactor, Chem. Eng. Sci. 49 (1994) 3257.
[16] V.Z. Yakhnin, A.B. Rovinsky, M. Menzinger, Differential-flow-induced pattern formation in the exothermic A → B reaction, J. Phys. Chem. 98 (1994) 2116.
[17] V.Z. Yakhnin, A.B. Rovinsky, M. Menzinger, Convective instability induced by differential transport in the tubular packed-bed reactor, Chem. Eng. Sci. 50 (1995) 2853.